

## Multidetector computerized tomographic fistulography in the evaluation of congenital branchial cleft fistulae and sinuses

Zhipeng Sun, MD, Kaiyuan Fu, DDS, PhD, Zuyan Zhang, DDS, PhD, MD, Yanping Zhao, and Xuchen Ma, DDS, PhD

**Objective.** The aim of this study was to primarily investigate the usefulness of computerized tomographic (CT) fistulography in the diagnosis and management of branchial cleft fistulae and sinuses.

**Study Design.** Fifteen patients with confirmed branchial fistulae or sinuses who had undergone CT fistulography were included. The diagnoses were confirmed by clinical, radiologic, or histopathologic examinations. The internal openings, distribution, and neighboring relationship of the lesions presented by CT fistulography were analyzed to evaluate the usefulness in comparison with x-ray fistulography.

**Results.** Nine patients were diagnosed with first branchial fistulae or sinuses, 2 with second branchial fistulae, and 4 with third or fourth branchial fistulae. The presence and location of the lesions could be seen on x-ray fistulography. The distribution of the lesions, internal openings, and neighboring relationship with parotid gland, carotid sheath, and submandibular gland could be clearly demonstrated on CT cross-sectional or volume-rendering images.

**Conclusions.** CT fistulography could provide valuable information and benefit surgical planning by demonstrating the courses of branchial anomalies in detail. (Oral Surg Oral Med Oral Pathol Oral Radiol 2012;113:688-694)

Branchial pouches and clefts begin to develop early in the fourth week of gestation and are gradually obliterated by surrounding mesenchyme to grow into the mature structures of the head and neck. Branchial anomalies, including cysts, fistulae, and sinuses are congenital malformations arising from abnormal persistence of branchial apparatus remnants during embryogenesis,<sup>1,2</sup> which can be classified into first, second, third, or fourth anomalies by identifying the course of the lesions via surgical or radiologic findings.<sup>2,3</sup> They can present as a sinus with a single opening on skin or mucosa, as a fistula when open communication between skin and internal mucosal surface is present, or as a cyst when no communication with skin or mucosa exists.<sup>4,5</sup>

It is common for branchial fistulae or sinuses to become inflamed, and significant morbidity may occur.<sup>6</sup> Complete excision of the entire fistulous or sinus tract is preferred for clinical management.<sup>6</sup> However, complex anatomic distribution often hampers the optimal exposure, dissection, and complete removal of the lesions. Surgical excision may be very difficult, and recurrence due to inadequate resection is frequent.

First branchial anomalies develop with a close relationship with the parotid gland, facial nerve, external

acoustic canal (EAC), and middle ear.<sup>2,4,7,8</sup> Second branchial anomalies pass close to the carotid sheath and glossopharyngeal and hypoglossal nerves and enter the pharynx via tonsillar fossa.<sup>2</sup> Third and fourth branchial anomalies arise from the piriform sinus of the hypopharynx and are collectively referred to as piriform sinus anomalies.<sup>9</sup> Third branchial anomalies pass deep to the internal carotid artery and glossopharyngeal nerve and course along the sternocleidomastoid muscle (SCM).<sup>10</sup> The fourth branchial anomalies pass in the tracheoesophageal groove into the mediastinum. They loop under the aortic arch on the left side and subclavian artery on the right.<sup>6,11</sup> Owing to the complicated anatomic neighboring relationship of the lesions, imaging evidence is needed both for diagnosis and surgical excision.

Ultrasound may be a first-line investigation without ionizing radiation; however, it is highly operator dependent and its success in imaging of sinuses and fistulae is variable.<sup>12,13</sup> Barium studies, fluoroscopy, or x-ray fistulography may confirm the presence of a tract, but cross-sectional imaging is still necessary to delineate the anatomic course for surgical considerations.<sup>13-16</sup> Magnetic resonance imaging (MRI) is superior in detecting branchial cysts but not constantly effective in delineation of the fistula.<sup>17-19</sup>

Computerized tomographic (CT) fistulography, with contrast media injected into the fistula, is promisingly effective in illustrating the lesion's spreading and anatomic relationship with adjacent structures. Several case reports have documented this technique.<sup>16,20</sup> The aim of present study was to primarily evaluate its effectiveness and usefulness in a large series of branchial anomalies.

Department of Oral and Maxillofacial Radiology, School and Hospital of Stomatology, Peking University, Beijing, China

Received for publication Aug 18, 2010; returned for revision Jul 23, 2011; accepted for publication Aug 30, 2011.

© 2012 Elsevier Inc. All rights reserved.

2212-4403/\$ - see front matter

doi:10.1016/j.oooo.2011.08.015

## MATERIALS AND METHODS

### Patients

Image data of 15 patients who had undergone CT fistulography because of branchial cleft fistulae or sinuses were retrospectively analyzed in present study. X-Ray fistulography had been performed in 10 patients. All of the patients and/or their legal guardians signed informed consents for the examination, and the study was performed in compliance with the policies of Institutional Review Board of Peking University.

The patients included 11 female and 4 male patients aging from 2 to 57 years old, with a median age of 16. The demographic information of the patients is summarized in Table I. The clinical, surgical, and radiographic data for the patients were examined to identify the embryologic derivation of the lesions.

### Techniques of CT fistulography

All examinations were performed when the inflammation processes were under control. Iodinated oil-soluble contrast medium (lipidol injection, 48 mg iodine/mL) was used. Iodine allergy tests were carried out before the examinations to avoid the allergic reaction caused by ionic iodinated contrast media.

The external opening of the skin was cannulated carefully with a 22-gauge blunt needle to probe the direction and depth of the tract. Next, the tract was irrigated with normal saline solution to remove the precipitated secretions. The contrast media was injected when the irrigation fluid became clear.

Enough contrast media should be injected to make sure that all branches of the fistula can be recorded. During injection, local swelling and pain may be present, and 3 children underwent the examinations under inhalation anesthesia (cases 1, 2, and 10). Radiation protective equipments, such as lead torso apron and gonad shielding, were used to reduce the effective radiation dose.

### CT scanning parameters and image postprocessing

CT examinations were performed using an 8-slice spiral CT machine of the GE Brightspeed Series. The spiral CT scans were carried out with the following parameters: 1.25 mm collimation; 16.75 mm/rotation table speed; 1:1.675 pitch. Automatic exposure control was used for radiation dose reduction. Noise index was controlled to  $>4.95$ . The voltage ranged from 80 to 120 kV and was adapted according to patient age and weight. Scan range was covered from the skull base to the level of the thoracic inlet.

Axial images with slice thickness of 1.25 mm were reconstructed for serial observation. Multiplanar reformation (MPR) images were regenerated in both sagittal

and coronal directions to analyze the fistulous extension. Volume-rendering (VR) and maximum-intensity projection (MIP) images were also acquired for direct visualization of the holistic course of the tracts.

### X-Ray fistulography

X-Ray fistulography had been performed in 10 patients (cases 4, 5, 7, 8, and 10-15). A combination of posterior-anterior and lateral projections was acquired.

Two experienced radiologists who were blinded to the clinical information were invited to assess all of the images. The following parameters were evaluated for comparison between CT and x-ray fistulography: presence and location of the fistula or sinus; classification; internal openings; and neighboring relationship with the parotid gland or carotid sheath.

## RESULTS

All of the patients complained of recurrent purulent discharge from skin openings in the head and neck region. The clinical and radiologic features are summarized in Table I. Except for 1 case (case 9), in which the lesion was present for 2 months, the other lesions were all congenitally acquired. Nine patients (cases 1-9) were diagnosed as first branchial fistulae or sinuses, 2 (cases 10 and 11) as second branchial fistula, and 4 (cases 12-15) as third or fourth branchial cleft fistula.

CT fistulography examinations were successfully performed in all of the patients, and no remarkable complications occurred. The presence, location, and classification of the lesions could be determined on x-ray fistulography in 10 cases. The internal openings, extension, and neighboring relationship of the lesions could be further illustrated on CT images.

As for the first branchial lesion, CT fistulography could accurately define the lesion's site within the parotid gland. The relationship with the facial nerve could be analyzed via retromandibular vein. In 9 cases of first branchial fistulae or sinuses, 4 lesions (cases 2 and 5-7) extended mostly in the superficial lobes (Figure 1, A-D) and 5 lesions (cases 1, 3, 4, 8, and 9) in the deep lobes of the parotid glands (Figure 1, E and F). Besides the external openings on the skin, internal openings in the EAC were found in 2 cases (cases 4 and 7). Intimate spatial relationship between the lesions and the EAC were seen in 6 cases (cases 2, 4, 5, and 7-9). Coexistence of cysts and sinuses were found in 2 cases (cases 1 and 3; Figure 2). X-Ray fistulography had been performed in 4 cases. The presence and location of the lesions within the parotid regions could be determined, but the information regarding their detailed distribution pattern within the parotid gland could not be observed in x-ray image.

In 2 cases (cases 10 and 11) of second branchial fistulae, the external openings located in the middle

**Table 1.** Clinical and radiologic presentations of 15 cases of branchial fistulae or sinuses

<i>Case no.</i>	<i>Sex</i>	<i>Age (y)</i>	<i>Side</i>	<i>External opening</i>	<i>Distribution of the contrast media</i>	<i>Internal opening</i>	<i>Diagnosis</i>
1	F	4	R	Hyoid bone level of anterior border of SCM	Upward into the deep lobe of the parotid gland, wrapping a cystic lesion in the deep lobe	None	First branchial sinus
2	F	4	R	Between the ear lobe and the mandibular angle	Upward into the superficial lobe of the parotid gland to the inferior wall of EAC	None	First branchial sinus
3	M	5	L	Hyoid bone level of anterior border of SCM	Upward in the deep lobe of the parotid gland and infuse into a cystic lesion slightly inferior to the parotid gland	None	First branchial sinus
4	F	13	L	Anterior border of SCM in the submandibular area	Upward into the deep lobe of the parotid gland and into the EAC	EAC	First branchial fistula
5	F	13	L	Between the earlobe and the mandibular angle	Into the superficial lobe of parotid gland and around the inferior wall of EAC	None	First branchial sinus
6	F	16	L	Between the earlobe and the mandibular angle	Into the superficial lobe of parotid gland	None	First branchial sinus
7	M	21	R	Between the earlobe and the mandibular angle	Upward into the superficial lobe of parotid gland and into the EAC	EAC	First branchial fistula
8	F	22	L	Mandibular angle	Upward into the deep lobe of parotid gland and into the inferior wall of EAC	None	First branchial sinus
9	F	57	R	Inferior to the mastoid tip	Into the deep lobe of parotid gland around the inferior wall of EAC	None	First branchial sinus
10	F	2	R	Hyoid bone level of anterior border of SCM	Upward into the tonsillar fossa	Tonsillar fossa	Second branchial fistula
11	M	13	L	Hyoid bone level of anterior border of SCM	Upward into the tonsillar fossa	Tonsillar fossa	Second branchial fistula
12	F	18	L	Inferior third of anterior border of SCM	Upward into the piriform sinus	Piriform sinus	Third or fourth branchial fistula
13	F	50	R	Inferior third of the anterior border of SCM	Upward into the piriform sinus	Piriform sinus	Third or fourth branchial fistula
14	M	16	L	Inferior third of the anterior border of SCM	Upward into the piriform sinus	Piriform sinus	Third or fourth branchial fistula
15	F	20	L	Inferior third of the anterior border of SCM close to the suprasternal notch	Upward into the piriform sinus	Piriform sinus	Third or fourth branchial fistula

SCM, Sternocleidomastoid muscle; EAC, external acoustic canal.

Figure 1. The extension of the tracts within the parotid glands in first branchial anomalies. **A, B**, Axial and coronal images showed the reticular tracts (*red arrows*) extending into the superficial lobe of parotid gland (case 5). **C, D**, The tracts (*red arrows*) could be seen in lateral and posterior-anterior projections of x-ray fistulography, but their extension area within the parotid gland could not be determined (case 5). **E, F**, Axial and coronal images showed the cylindrical tract (*red arrows*) course into the deep lobe of parotid gland (case 8). The tract coursed beneath the retromandibular vein (*yellow arrow*), which is deep to the facial nerve. **G, H**, The site of the tract (*red arrows*) within the parotid gland could not be determined in x-ray fistulography (case 8).

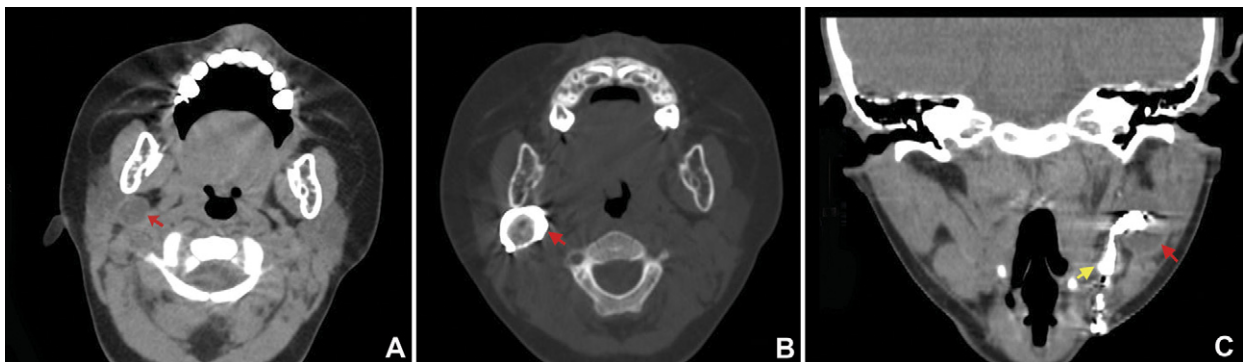


Figure 2. Coexistence of cysts and sinuses in first branchial lesions. **A**, Axial images showed the cystic lesion (*red arrow*) in the deep lobe of right parotid gland (case 1). **B**, The cystic lesion was encapsulated by the contrast media, indicating that the sinus is not communicating with the cyst (case 1). **C**, CT fistulography (coronal image) showed that the sinus (*yellow arrow*) fused into a cystic lesion (*red arrow*) in the deep lobe of the right parotid gland (case 3).

third of the anterior border of the SCM (Figure 3, A), the tracts coursed beneath the submandibular gland and anterior to the carotid sheath (Figure 3, B and C), and the internal openings were found in the tonsillar fossae on ipsilateral side (Figure 3, D). On X-ray fistulography, the tracts could be seen in the upper neck region, but the anatomic relationship between the soft tissue and the internal openings could not be determined.

Four cases (cases 12-15) were diagnosed as third or fourth branchial fistulae, which extended along the

anterior border and into the deep side of the SCM. The presence of internal openings in the piriform sinuses on the ipsilateral side could be determined in all of the cases (Figure 4). On x-ray fistulography, the tracts could be seen in the lower neck region, and extension could be observed; however, the soft-tissue neighboring relationship and the internal openings could not be determined.

Eight patients (cases 2-4, 6-8, 12, and 14) had undergone surgical excision of the lesions, and the histopathologic examinations confirmed the diagnoses.

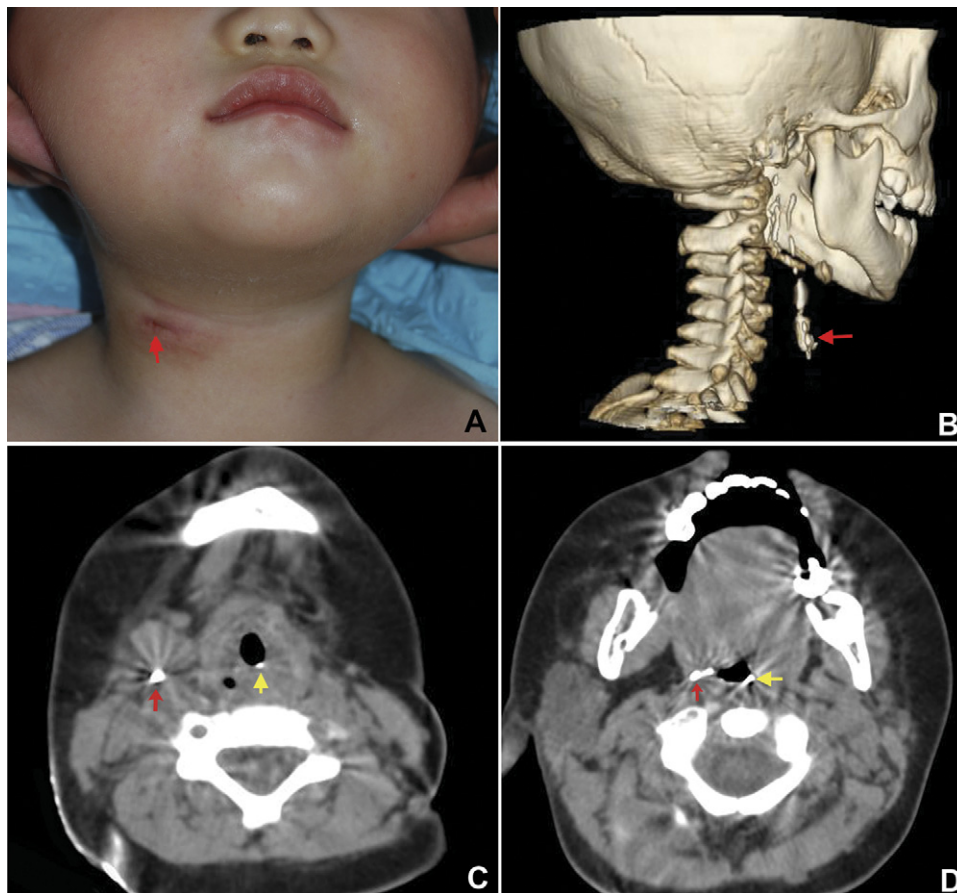


Figure 3. CT fistulography in the second branchial cleft fistula. **A**, The external opening (case 10) located in the middle third of the anterior border of SCM (red arrow). **B**, Volume-rendering image showed the holistic view of the tract (red arrow). **C**, The tract (red arrow) coursed beneath the submandibular gland and anterior to the carotid sheath. **D**, The contrast media leaked into the trachea (yellow arrow) via the internal opening in the piriform sinus (red arrow). (Image is available in color at [www.ooooe.net](http://www.ooooe.net)).

## DISCUSSION

Compared with x-ray fistulography, CT could provide more valuable information about the lesions. Knowledge of the extension of the lesions and their relationship to surrounding structures is of utmost significance for diagnosis and surgical excision. The superficial or deep lobe of the parotid gland, the facial nerve, and the EAC were frequently involved in the first branchial anomalies. The submandibular gland, carotid sheath and the SCM usually have close anatomic relationship with the second, third, or fourth branchial lesions. Understanding of this anatomy is essential in preventing injuries during resection.

CT fistulography provides detailed understanding in branchial anomalies. Fully implementing the volume data by various imaging postprocessing techniques, such as MPR and VR, optimizes the visualization of the lesions. Detailed anatomy could be seen with the thin-slice cross-sectional images and nearly isotropic MPR images. Thick-slice MIP images also help in demon-

strating the internal opening. VR images best illustrate the whole view of the tract 3 dimensionally and are also useful for diagnosis and surgical planning.

Information based on history and clinical examination may not be difficult for making the diagnosis. Small skin openings on the face or neck may be discovered at birth and present for decades.<sup>13</sup> The patients may be asymptomatic for a long time, or only occasional drainage from the skin opening is noticed. Infection may occur frequently and purulent discharge is common. Infection may be secondary to upper respiratory inflammation and closely associates with the gathering of the secretion. Once infection occurs, it may be recurrent and last for decades. Laryngoscope helps in identifying internal opening in the tonsillar fossa or piriform sinus.<sup>13</sup> Surgical removal may be difficult, and inadequate resection of the lesion is likely to cause recurrence.<sup>4</sup>

Based on the knowledge of embryologic derivatives of the branchial apparatus, the internal openings of

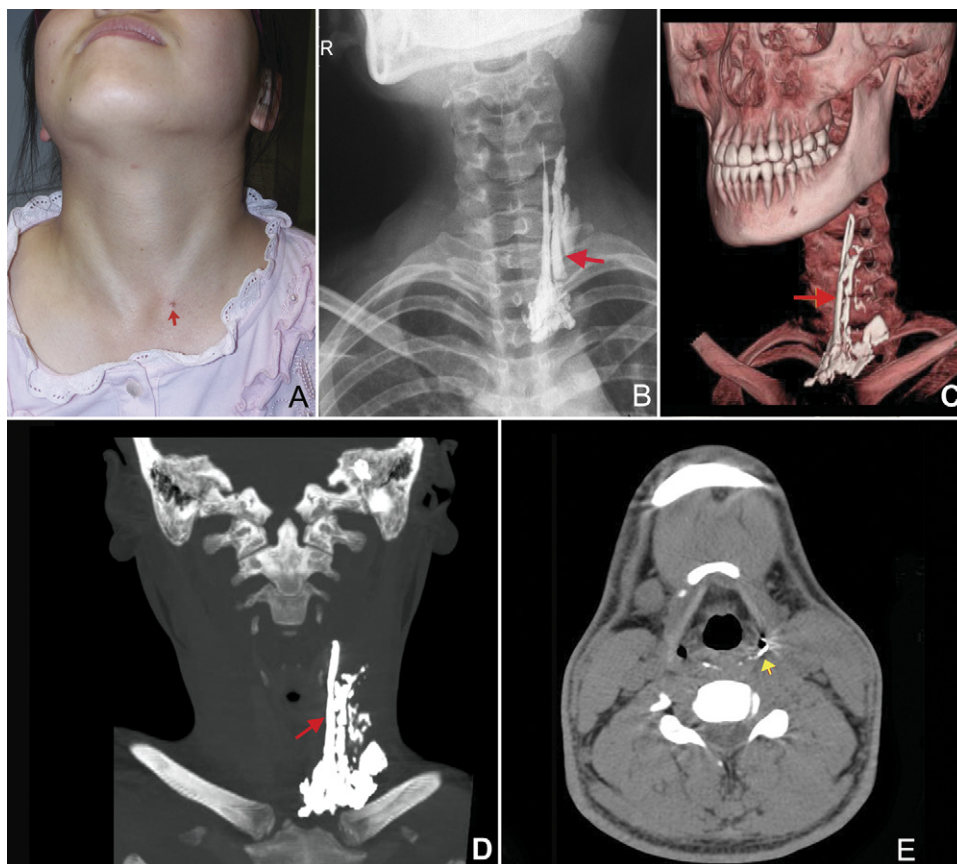


Figure 4. CT fistulography in the third or fourth branchial cleft fistula. **A**, The external opening (case 15) located in the inferior end of the anterior border of SCM (red arrow). **B, C**, X-Ray fistulography (B) and volume-rendering image (C) showed that the fistula (red arrows) extended upward to the level of hyoid bone. **D, E**, Coronal maximum-intensity projection image (D, 15-mm thickness) and axial image (E) showed the fistula (red arrow) coursing upward into the piriform sinus (yellow arrow). (Image is available in color at [www.ooooe.net](http://www.ooooe.net)).

these anomalies are predictable and crucial for clinical diagnosis. During normal development, the first branchial arch forms the mandible and a portion of the maxillary process of the upper jaw. This arch is also involved in development of portions of the inner ear, whereas the cleft and pouch become part of the EAC, eustachian tube, middle ear cavity, and mastoid air cells. Two types of first branchial cleft anomalies have been documented.<sup>5</sup> Type I are derived from buried cell rests of the first branchial cleft, resulting in an intraparotid cyst or sinus without communication with the external auditory canal. Type II anomalies are thought to occur as a result of incomplete closure of the first branchial cleft, resulting in a cyst or a sinus inferior to the parotid gland that may communicate with the EAC.<sup>5</sup>

Coexistence of cyst and sinus was seen in 2 cases of the first branchial anomalies. In case 1, the cyst was located inside the deep lobe of the parotid gland (type I lesion) and wrapped by the injected contrast media. In case 3, the cyst was located slightly inferior to the

parotid gland (type II lesion) and the contrast media extended along the sinus fusing into the cyst. CT and MRI are preferred for the diagnosis of the branchial cyst. On CT images, these lesions present as thin-walled cystic lesions, which are most often located along the anterior aspect of the SCM and show homogeneously low attenuation with little peripheral enhancement.

The first branchial anomalies can be variably associated with the facial nerve. They may develop medially, laterally to the facial nerve, or between the marginal branches.<sup>8</sup> A safe complete resection requires a full exposure of the facial nerve. Although it is difficult for CT to illustrate the facial nerves in the parotid glands in axial images directly, the relationship between the lesions and the retromandibular vein can be used for analysis, because facial nerves branch constantly superficially to the retromandibular vein.

The second arch contributes to the hyoid bone and adjacent area of the neck. The second pouch gives rise

to the palatine tonsil and tonsillar fossa. Sometimes differentiation between the first and second branchial cleft anomalies may be difficult clinically, because the external openings in these 2 circumstances may be very close. The second branchial anomalies usually enter the tonsillar fossa on the ipsilateral side. It is the internal opening of the fistula that is crucial in defining the cleft or pouch of origin.

External openings of the third and fourth branchial sinuses or fistulae locate along the inferior third of the anterior border of SCM. Differentiation between the third or fourth anomalies may be very difficult. Theoretically, the tract of a third branchial anomaly should pass superiorly to the hypoglossal nerve. The tract of a fourth branchial anomaly should pass inferiorly to the remnants of the fourth arch arteries (the subclavian artery on the right and the aortic arch on the left).<sup>9</sup> Although classic courses of the third and fourth fistulae or sinuses have been widely quoted in the literature, cases matching these descriptions are rare.<sup>9</sup> It is suggested that these lesions should be generally considered as branchial anomalies of the piriform fossa based on anatomical considerations to avoid confusion about the embryologic derivation.<sup>9,21</sup>

Complete excision of these lesions is required to prevent recurrence. Methylene blue can be injected into the tract during the operation to demarcate the sinuses or fistulae.<sup>22</sup> Potential risk of nerve injury should be avoided as a complication of surgical excision.<sup>4</sup> The information acquired from CT fistulography is helpful in surgical planning.

In conclusion, CT fistulography presented an effective alternative imaging protocol supplemental to ultrasonography, MRI, and x-ray in the radiologic evaluation of the branchial fistulae or sinuses.

## REFERENCES

1. Triglia JM, Nicollas R, Ducroz V, Koltai PJ, Garabedian EN. First branchial cleft anomalies: a study of 39 cases and a review of the literature. *Arch Otolaryngol Head Neck Surg* 1998;124:291-5.
2. Waldhausen JH. Branchial cleft and arch anomalies in children. *Semin Pediatr Surg* 2006;15:64-9.
3. Benson MT, Dalen K, Mancuso AA, Kerr HH, Cacciarelli AA, Mafee MF. Congenital anomalies of the branchial apparatus: embryology and pathologic anatomy. *Radiographics* 1992;12:943-60.
4. d'Souza AR, Uppal HS, De R, Zeitoun H. Updating concepts of first branchial cleft defects: a literature review. *Int J Pediatr Otorhinolaryngol* 2002;62:103-9.
5. Mukherji SK, Fatterpekar G, Castillo M, Stone JA, Chung CJ. Imaging of congenital anomalies of the branchial apparatus. *Neuroimaging Clin N Am* 2000;10:75-93.
6. Nicoucar K, Giger R, Pope HG Jr, Jaecklin T, Dulguerov P. Management of congenital fourth branchial arch anomalies: a review and analysis of published cases. *J Pediatr Surg* 2009;44:1432-9.
7. May M, d'Angelo AJ Jr. The facial nerve and the branchial cleft: surgical challenge. *Laryngoscope* 1989;99:564-5.
8. Solares CA, Chan J, Koltai PJ. Anatomical variations of the facial nerve in first branchial cleft anomalies. *Arch Otolaryngol Head Neck Surg* 2003;129:351-5.
9. James A, Stewart C, Warrick P, Tzifa C, Forte V. Branchial sinus of the piriform fossa: reappraisal of third and fourth branchial anomalies. *Laryngoscope* 2007;117:1920-4.
10. Nicoucar K, Giger R, Jaecklin T, Pope HG Jr, Dulguerov P. Management of congenital third branchial arch anomalies: a systematic review. *Otolaryngol Head Neck Surg*;142:21-8 e2.
11. Rea PA, Hartley BE, Bailey CM. Third and fourth branchial pouch anomalies. *J Laryngol Otol* 2004;118:19-24.
12. Park SW, Han MH, Sung MH, Kim IO, Kim KH, Chang KH, Han MC, et al. Neck infection associated with pyriform sinus fistula: imaging findings. *AJNR Am J Neuroradiol* 2000;21:817-22.
13. Shrime M, Kacker A, Bent J, Ward RF. Fourth branchial complex anomalies: a case series. *Int J Pediatr Otorhinolaryngol* 2003;67:1227-33.
14. Shin LK, Gold BM, Zelman WH, Katz DS. Fluoroscopic diagnosis of a second branchial cleft fistula. *AJR Am J Roentgenol* 2003;181:285.
15. Seki N, Himi T. Retrospective review of 13 cases of pyriform sinus fistula. *Am J Otolaryngol* 2007;28:55-8.
16. Whetstone J, Branstetter BF, Hirsch BE. Fluoroscopic and CT fistulography of the first branchial cleft. *AJNR Am J Neuroradiol* 2006;27:1817-9.
17. Black CJ, O'Hara JT, Berry J, Robson AK. Magnetic resonance imaging of branchial cleft abnormalities: illustrated cases and literature review. *J Laryngol Otol* 2010;124:213-5.
18. Mukherji SK, Tart RP, Slattey WH, Stringer SP, Benson MT, Mancuso AA. Evaluation of first branchial anomalies by CT and MR. *J Comput Assist Tomogr* 1993;17:576-81.
19. Keogh IJ, Khoo SG, Waheed K, Timon C. Complete branchial cleft fistula: diagnosis and surgical management. *Rev Laryngol Otol Rhinol (Bord)* 2007;128:73-6.
20. Ryu CW, Lee JH, Lee HK, Lee DH, Choi CG, Kim SJ. Clinical usefulness of multidetector CT fistulography of branchial cleft fistula. *Clin Imaging* 2006;30:339-42.
21. Mouri N, Muraji T, Nishijima E, Tsugawa C. Reappraisal of lateral cervical cysts in neonates: pyriform sinus cysts as an anatomy-based nomenclature. *J Pediatr Surg* 1998;33:1141-4.
22. Dickson JM, Riding KH, Ludemann JP. Utility and safety of methylene blue demarcation of preauricular sinuses and branchial sinuses and fistulae in children. *J Otolaryngol Head Neck Surg*. 2009. 38: 302-10.

## Reprint requests:

Dr. Xuchen Ma  
 Department of Oral and Maxillofacial Radiology  
 Center for Temporomandibular Disorders and Orofacial Pain  
 School and Hospital of Stomatology  
 Peking University  
 #22 ZhongGuanCun South Street  
 Haidian District  
 Beijing 100081  
 China  
 kqxcma@bjmu.edu.cn